Confirmation of a large density variation along the magnetic axis of the Columbia Non-neutral Torus

Michael Hahn, Thomas Sunn Pedersen, Quinn Marksteiner, and John W. Berkery
Department of Applied Physics and Applied Mathematics, Columbia University, New York, New York 10027, USA

(Received 19 September 2007; accepted 21 January 2008; published online 27 February 2008)

Significant variations in the density and potential along the axis of a pure electron plasma in the Columbia Non-neutral Torus (CNT) stellarator have now been measured. Large variations along the magnetic field are predicted by three-dimensional equilibrium reconstructions of CNT plasmas and by simple electrostatic and geometric arguments [Lefrancois and Pedersen, Phys. Plasmas **13**, 120702 (2006)]. The density variation, $n_{\mathrm{axis},\phi=0^\circ}/n_{\mathrm{axis},\phi=90^\circ}$, is measured directly for several different plasma equilibria, and has a median value of 7.8, consistent with the predicted density variation of 4.4, because the error bars are large. The associated variation in potential predicted from the Boltzmann relation, $e\Delta\Phi/T_e=\ln(4.4)=1.5$, was also measured experimentally. The median measured, $e\Delta\Phi/T_e$, was 1.1, which is of the predicted sign and in rough agreement with the measurements, but smaller than predicted. The difference is statistically significant, but might be related to the imperfect numerical modeling of the complicated electrostatic boundary conditions in CNT. The measured variations reconfirm that the Debye lengths of these plasmas are small. © *2008 American Institute of Physics*. [DOI: 10.1063/1.2844439]

Non-neutral plasmas display a host of the collective plasma behaviors seen in neutral plasmas such as Debye shielding[1] and plasma waves.[1–3] At the same time, non-neutral plasmas have unique properties that clearly distinguish them from quasineutral plasmas. For example, in Penning traps essentially infinite confinement times and relaxation to global thermal equilibrium have been observed[4] and are understood theoretically by considering the conservation of canonical angular momentum.[1,5,6]

Another unique feature of non-neutral plasmas is that for certain confinement geometries there can be a large density variation along the magnetic field even when the plasma is in equilibrium. This was first demonstrated by Fajans[7] in the cylindrical mirror configuration where the density varies in proportion to the magnetic field strength. Such density and potential variations have important effects on the plasma, for example a potential variation causes electrostatic trapping of particles.

The size of the axial density variation in a non-neutral plasma depends on the structure of the magnetic field and the Debye length of the plasma. In a toroidally symmetric device[8–11] or a large Debye length plasma, there is no variation along the magnetic axis. In the large Debye length, non-neutral plasmas in the Compact Helical System (CHS) experiment density and potential variations have been observed to be greater on the outer surfaces than on the inner surfaces.[12] The variations in CHS are caused by the nonconforming electrostatic boundary and ineffective screening in the large Debye length plasma. In the Columbia Non-neutral Torus (CNT), the density variation on the magnetic axis is robustly present in the small Debye length limit and is largely independent of boundary conditions. Numerical equilibrium solutions show that a flux surface conforming electrostatic boundary will actually increase the density variation on axis, whereas in CHS plasmas such a boundary would nearly eliminate the variation of density and potential on the outer surfaces and the variation on axis would remain negligible.

The CNT[13] has a large toroidal variation in the shape of the magnetic surfaces and the magnetic field strength (Fig. 1). There are significant differences in the cross-sectional shape of the magnetic surfaces at the $\phi=0^\circ$ (thin) and $\phi=90^\circ$ (thick) locations, which correspond to the high and low field points along the magnetic axis, respectively (Fig. 2). The magnetic field strength along the magnetic axis varies by a factor of 1.8. Typical plasmas in CNT have a temperature of 5 eV and a density on the order of 10^{12} m^{-3} giving a Debye length of 1.5 cm.[14] The minor radius of the device is about 15 cm, or 10 Debye lengths, so these are small Debye length plasmas. These characteristics permit CNT plasmas to exhibit a large density variation along the magnetic axis.

Computational results from a numerical routine (PBS) that solves the Poisson–Boltzmann equilibrium equation in the magnetic surface geometry of CNT[15] predicted a factor of $n_{\mathrm{axis},\phi=0^\circ}/n_{\mathrm{axis},\phi=90^\circ}=5.3$ density variation along the magnetic axis of the plasma.[16]

This density variation, which is much larger than the magnetic field strength variation, was explained by the geometric differences between the $\phi=0^\circ$ and 90° cross sections and is developed in detail in Ref. 16. In the cold plasma limit, the potential drop across the surfaces, $\Delta\Phi_\perp$, is a constant $\Delta\Phi_{\perp,\phi=0^\circ}/\Delta\Phi_{\perp,\phi=90^\circ}=1$. Then $n_{\mathrm{axis},\phi=0^\circ}$ can be related to $n_{\mathrm{axis},\phi=90^\circ}$ through Poisson's equation. The density ratio will be the ratio of two integrals that depend on the geometry of each cross section and the radial density profile. The $\phi=0^\circ$ cross section can be approximated as a slab, while the $\phi=90^\circ$ cross section can be approximated as a cylinder (Fig. 2). It turns out that the dependence on the radial density

FIG. 1. (Color online) Cutaway view of the CNT magnetic surface configuration. The average major radius of the plasma is ≈30 cm and the average minor radius is ≈15 cm.

profile is weak compared to the dependence on the geometry, and one finds that $n_{\text{axis},\phi=0^\circ}/n_{\text{axis},\phi=90^\circ} \approx \frac{1}{2}(a/w_{1/2})^2$, where $a \approx 18.0$ cm is the radius of the $\phi=90^\circ$ cross section and $w_{1/2} \approx 5.6$ cm is the half-width of the $\phi=0^\circ$ cross section. This geometric argument predicts a factor of 5.2 density variation, in agreement with the numerical equilibrium model using the actual magnetic surface geometry.

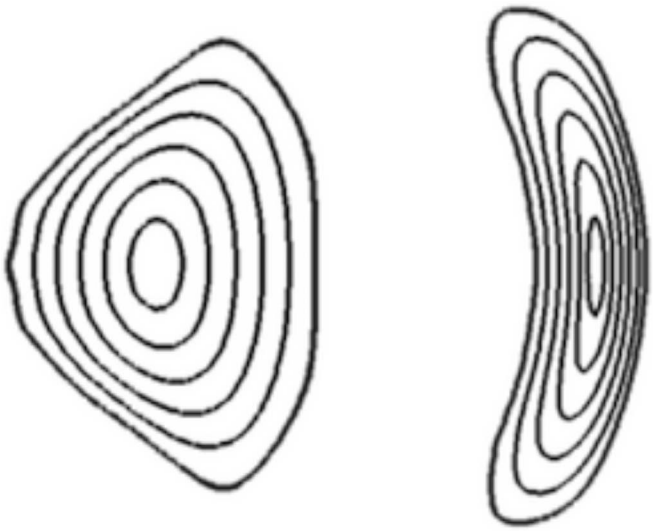

FIG. 2. Numerically calculated magnetic surface contours of the thick cross section at $\phi=90^\circ$ (left) and the thin cross section at $\phi=0^\circ$ (right). Compare to Fig. 1.

FIG. 3. (Color online) CAD drawing of the CNT device showing the complex boundary conditions set by the grounded vacuum chamber and coils.

For a Boltzmann distribution of electrons, the density variation along the axis is related to the potential variation by

$$\Phi_{\text{axis},\phi=0^\circ} - \Phi_{\text{axis},\phi=90^\circ} = \frac{T_e}{e} \ln\left(\frac{n_{\text{axis},\phi=0^\circ}}{n_{\text{axis},\phi=90^\circ}}\right). \quad (1)$$

Defining $\Delta\Phi \equiv \Phi_{\text{axis},\phi=0^\circ} - \Phi_{\text{axis},\phi=90^\circ}$ and using Eq. (1), the potential variation in CNT is predicted to be $\Delta\Phi = 1.65\, T_e/e$.

These predictions assume that the plasma is surrounded by a conforming equipotential boundary. In reality, the plasma boundary conditions are determined by the coils and vacuum chamber (Fig. 3). An approximation to these boundary conditions has been implemented in the numerical code and results in a slightly smaller predicted variation of $n_{\text{axis},\phi=0^\circ}/n_{\text{axis},\phi=90^\circ} = 4.4$ and $\Delta\Phi = 1.5\, T_e/e$.[16] This paper presents the experimental verification of large density and potential variations and a quantitative comparison between the measured and predicted values.

Experimental measurements are performed with emissive and Langmuir probes.[17] The plasma potential is measured as the voltage at which the current-voltage characteristic of an emissive (hot) probe deviates from the characteristic of the same probe in the same location, but nonemissive (cold).[17,18] We refer to the hot and cold states of the probe as "the emissive probe" and "the Langmuir probe." When the probe potential is less negative than the plasma potential, the emissive probe collects the same current as the Langmuir probe except for an offset caused by the finite heating voltage drop across the hot filament. The procedure for determining the plasma potential is to subtract the offset and then locate the point where $I_{\text{emissive}} - I_{\text{Langmuir}}$ becomes negative.

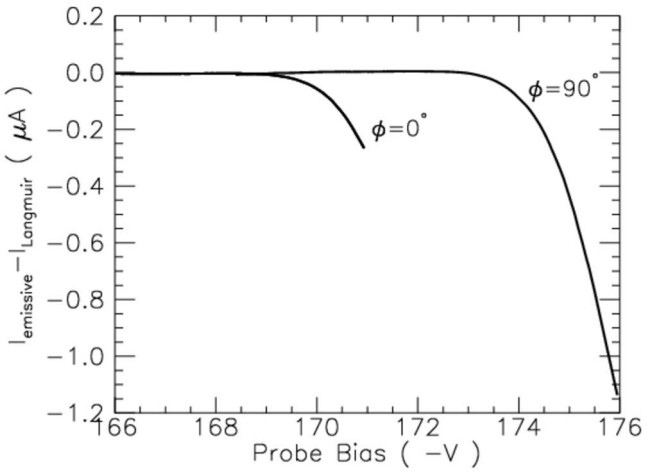

FIG. 4. The difference between the emissive and Langmuir probe characteristics is plotted as a function of the probe bias for probes at the $\phi=0°$ and 90° cross sections. The points where $I_{\text{emissive}}-I_{\text{Langmuir}}$ becomes negative are the plasma potentials. There is clearly a potential difference between the two locations. For comparison with Table I, this is the 170 V emitter bias and temperature is $T_e=3.6\pm0.6$ eV.

The temperature and density are found from a fit of the Langmuir characteristic in the retarding region. If the current-voltage characteristic is plotted on a semilog plot, a linear fit can be done. The slope gives the electron temperature. The density is proportional to the exponential of the intercept of the fit with the plasma potential. The calculation of the density from the Langmuir probe characteristic depends on the exponential of the measured quantity leading to large asymmetric uncertainties in the density measurements. These procedures and associated uncertainty analysis are described more fully along with example I-V characteristics in Ref. 17.

Measurements of plasma potential, temperature, and density were done at the $\phi=0°$ and $\phi=90°$ cross sections. The plasma was created by a heated biased filament at the axis of the $\phi=0°$ cross section. Another filament at the axis of the $\phi=0°$ cross section and one on the axis of the $\phi=90°$ cross section were used as probes. The probes are held in place by insulating rods, which are known to perturb the plasma equilibrium. For consistency, the configuration of the rods was not changed during the experiment.

Different plasma equilibria were sampled by changing the emitter bias, which sets the plasma potential on the axis. The density scales linearly with the emitter bias, and the temperature tends to increase with emitter bias. The theory predicts that for small Debye length plasmas, the normalized axial variations ($e\Delta\Phi/T_e$, $n_{\text{axis},\phi=0°}/n_{\text{axis},\phi=90°}$) will be independent of emitter bias,[16] and measurements showed that these plasmas had small Debye lengths for each emitter bias used. The equilibrium and confinement properties of plasmas in CNT under similar conditions were reported in Refs. 17 and 19.

Clear variations in the potential (Fig. 4) and density were measured. For every measurement, the potential at the $\phi=90°$ cross section was always more negative and the density always less than at the $\phi=0°$ cross section (Table I). As predicted, there was no statistically significant trend as a function of the emitter bias.

Poisson's equation implies that since the potential difference along the axis between $\phi=0°$ and $\phi=90°$ (≈4 V) is small compared to the potential drop across the surfaces and there are significant geometric differences between the two locations, there must be a large density variation between those cross sections. If the plasma is in a Boltzmann distribution, the size of this small potential difference is a measure of the density variation Eq. (1).

To make a quantitative comparison with theory, we performed a careful uncertainty analysis taking into account statistical uncertainties in the measurements and systematic uncertainties in the alignment of the probes. A Monte Carlo error analysis was used to determine the density and potential variations and associated uncertainties without assuming a probability distribution function, such as the standard Gaussian. Table I records the median and the 68% (1σ) and 95% (2σ) probability regions about the median.

The probes were aligned on the axis with an estimated accuracy of $\Delta\Psi\lesssim0.04$, that is, about 1 cm in real space. Ψ is a coordinate that labels the magnetic surfaces so that $\Psi=0$ at the axis and $\Psi=1$ at the last closed flux surface. This translates to an uncertainty $\lesssim0.3$ V in the measured probe potential, estimated from equilibrium reconstructions based on measured profiles of a −200 V plasma. The uncertainty in toroidal location of the measurement, on the order of a few degrees, led to much smaller uncertainties in voltage. Asso-

TABLE I. Summary of measured potential and density variations along the magnetic axis for various emitter bias values and the 1σ (68%) and 2σ (95%) confidence intervals.

Bias	T_e	$e\Delta\Phi/T_e$			$n_{\phi=0°}/n_{\phi=90°}$		
		Median	1σ	2σ	Median	1σ	2σ
170 V	3.6 ± 0.6	1.1	1.0–1.4	0.8–1.6	5.3	3.7–8.5	2.4–15.5
200 V	3.6 ± 0.5	1.3	1.2–1.6	1.1–2.0	10.7	6.2–23.4	3.7–47.1
230 V	3.9 ± 1.0	0.8	0.7–1.0	0.6–1.6	27.8	13.5–60.3	4.0–197.4
260 V	6.5 ± 1.3	0.7	0.6–1.1	0.5–1.3	8.1	4.3–16.5	3.1–31.2
290 V	5.3 ± 0.7	1.1	1.0–1.3	0.9–1.5	4.6	2.4–13.0	1.4–32.1
Average		1.1	0.7–1.3	0.6–1.7	7.8	3.8–20.0	2.1–55.1

ciated uncertainties in density were also taken into account in the Monte Carlo calculations.

An average value for the variations was found by combining the Monte Carlo generated values for the different biases into a composite distribution. The result is an axial variation in potential with a 1σ range of $\Delta\Phi=0.7-1.3\ T_e/e$ and a median of $\Delta\Phi=1.1\ T_e/e$. The resulting 1σ range for $n_{\mathrm{axis},\phi=0^\circ}/n_{\mathrm{axis},\phi=90^\circ}$ is 3.8–20.0 with a median value of 7.8. The density variation is roughly consistent with the theoretically predicted value, and the potential variation is smaller than predicted. There is better than 95% confidence that the density on the axis at $\phi=0^\circ$ is at least twice the density at $\phi=90^\circ$. Thus, direct measurements show that the density variation is larger than the magnetic field strength variation of $B_{\max}/B_{\min}=1.8$. Potential variation along the axis has also been clearly measured. The measured value of $\Delta\Phi=1.1\ T_{e/e}$ is of the expected sign and roughly the right magnitude, but is smaller than predicted ($\Delta\Phi=1.5\ T_e/e$). The predicted value falls outside the 1σ interval of the measurements, but inside the 2σ interval. Thus, the discrepancy is large enough that it should be considered a real discrepancy, although it is still within 2σ of the measured one, so it is not a glaring discrepancy.

Theory assumes that the parallel electron distribution function is Maxwellian and consequently predicts a Boltzmann density distribution along the magnetic field in equilibrium. A Maxwellian is consistent with measurements made with Langmuir probes in CNT.[14,17] The Langmuir probes measure the parallel distribution function since the electrons are well magnetized and are being collected along the field. Thus, the theory and experiment should agree even if the perpendicular temperature, which has not been measured in CNT, is different from the parallel temperature.

The source of the discrepancy may be the boundary conditions in the numerical modeling (Fig. 3). For the nonconforming boundary case (the present experimental situation), the boundary conditions are crudely modeled by static charge distributions on the computational grid. This model makes approximations that cause the numerical conditions to differ from the experimental conditions, such as a spherical vacuum chamber and a sinusoidal image charge distribution on the coils. The PBS code shows that a nonconforming boundary similar to the actual boundary does reduce the size of $e\Delta\Phi/T_e$ compared to its value with the conforming boundary. A more accurate representation of the present boundary condition in the PBS code could give a result that is in significantly better agreement.

The predicted large potential and density variation along the magnetic axis in the Columbia Non-neutral Torus has been confirmed experimentally. The density is less and the potential correspondingly more negative at the $\phi=90^\circ$ than at the $\phi=0^\circ$ cross section. Direct measurements of the density variation show that it is larger than the magnetic field strength variation and is consistent with the values predicted numerically and analytically for a small Debye length plasma in CNT. The potential variation is of the predicted sign, but somewhat smaller than predicted. The small value of the potential variation along the field (about 5 V), relative to the radial potential drop in CNT (about 200 V), is confirmation that the Debye length in CNT is small, as previously established with direct probe measurements.[14] The large density variation along the magnetic field is further proof that the Debye length is small.

This work is supported by the NSF CAREER program, Grant No. NSF-PHY-04-49813, and the Fusion Energy Sciences Postdoctoral Research Program of the U.S. Department of Energy.

[1] R. C. Davidson, *Physics of Nonneutral Plasmas* (Imperial College Press, London, 2001), p. 59.
[2] S. A. Prasad and T. M. O'Neil, Phys. Fluids **26**, 665 (1983).
[3] F. Anderegg, N. Shiga, J. R. Danielson, D. H. E. Dubin, C. F. Driscoll, and R. W. Gould, Phys. Rev. Lett. **90**, 115001 (2003).
[4] C. F. Driscoll, J. H. Malmberg, and K. S. Fine, Phys. Rev. Lett. **60**, 1290 (1988).
[5] T. M. O'Neil, Phys. Fluids **23**, 2216 (1980).
[6] T. M. O'Neil and C. F. Driscoll, Phys. Fluids **22**, 266 (1979).
[7] J. Fajans, Phys. Plasmas **10**, 1209 (2003).
[8] K. Avinash, Phys. Fluids B **3**, 3226 (1991).
[9] J. D. Daugherty, J. E. Eninger, and G. S. Janes, Phys. Fluids **12**, 2677 (1969).
[10] P. Zaveri, P. I. John, K. Avinash, and P. K. Kaw, Phys. Rev. Lett. **68**, 3295 (1992).
[11] M. R. Stoneking, P. W. Fontana, R. L. Sampson, and D. J. Thuecks, Phys. Plasmas **9**, 766 (2002).
[12] H. Himura, H. Wakabayashi, Y. Yamamoto, M. Isobe, S. Okamura, K. Matsuoka, A. Sanpei, and S. Masamune, Phys. Plasmas **14**, 022507 (2007).
[13] T. S. Pedersen, J. P. Kremer, R. G. Lefrancois, Q. Marksteiner, N. Pomphrey, W. Reiersen, F. Dahlgreen, and X. Sarasola, Fusion Sci. Technol. **50**, 372 (2006).
[14] J. P. Kremer, T. S. Pedersen, R. G. Lefrancois, and Q. Marksteiner, Phys. Rev. Lett. **97**, 095003 (2006).
[15] R. G. Lefrancois, T. S. Pedersen, A. H. Boozer, and J. P. Kremer, Phys. Plasmas **12**, 072105 (2005).
[16] R. G. Lefrancois and T. S. Pedersen, Phys. Plasmas **13**, 120702 (2006).
[17] J. P. Kremer, T. S. Pedersen, Q. Marksteiner, R. G. Lefrancois, and M. Hahn, Rev. Sci. Instrum. **78**, 013503 (2007).
[18] N. Hershkowitz and M. H. Cho, J. Vac. Sci. Technol. A **6**, 2054 (1988).
[19] J. W. Berkery, T. S. Pedersen, J. P. Kremer, Q. R. Marksteiner, R. G. Lefrancois, M. S. Hahn, and P. W. Brenner, Phys. Plasmas **14**, 062503 (2007).